Analysis and Evaluation of IKONOS Image Fusion Algorithm Based on Land Cover Classification

Xia JING[1]*, Yan BAO[2]*

1. College of Geometrics, Xian University of Science and Technology, Xi'an 710054, China; 2. The Key Laboratory of Urban Security and Disaster Engineering, Ministry of Education, Beijing 100124, China

Abstract Different fusion algorithm has its own advantages and limitations, so it is very difficult to simply evaluate the good points and bad points of the fusion algorithm. Whether an algorithm was selected to fuse object images was also depended upon the sensor types and special research purposes. Firstly, five fusion methods, *i. e.* IHS, Brovey, PCA, SFIM and Gram-Schmidt, were briefly described in the paper. And then visual judgment and quantitative statistical parameters were used to assess the five algorithms. Finally, in order to determine which one is the best suitable fusion method for land cover classification of IKONOS image, the maximum likelihood classification (MLC) was applied using the above five fusion images. The results showed that the fusion effect of SFIM transform and Gram-Schmidt transform were better than the other three image fusion methods in spatial details improvement and spectral information fidelity, and Gram-Schmidt technique was superior to SFIM transform in the aspect of expressing image details. The classification accuracy of the fused image using Gram-Schmidt and SFIM algorithms was higher than that of the other three image fusion methods, and the overall accuracy was greater than 98%. The IHS-fused image classification accuracy was the lowest, the overall accuracy and kappa coefficient were 83.14% and 0.76, respectively. Thus the IKONOS fusion images obtained by the Gram-Schmidt and SFIM were better for improving the land cover classification accuracy.

Key words IKONOS image, Fusion algorithm, Comparison, Evaluation, Land cover classification, Accuracy

1 Introduction

The image fusion can produce multi-spectral and high spatial resolution image to achieve the complementation between a variety of information resources, raise people's awareness of remote sensing data, and increase the decision-making scientificity and accuracy [1]. Currently most of the studies of remote sensing image fusion algorithm focus on selecting suitable fusion algorithm based on the type of sensor or improving the original image algorithm in order to improve the quality of fusion image. These studies rarely consider the application purpose. Zhang Ningyu *et al.* use Brovey fusion and wavelet fusion to analyze the impact on the amount of information of QuickBird image, and find that the Brovey fusion method does not apply to the processing of QuickBird remote sensing image [2]. Li Chunhua *et al.* perform the quantitative analysis of the spectral fidelity and high frequency information integration, and find that the fusion algorithm based on statistical theory is in general better than the fusion method based on filtering principle, so it is more suitable for the fusion of QuickBird high-resolution image [3]. To minimize the spectral distortion of IKONOS 1-m fusion image, Kalpoma KA and Kudoh J use the steepest descent method to establish the spectral response relationship between panchromatic band and multispectral image band [4]. Liu Jun *et al.* develop a remote sensing image fusion method for fast discrete Curvelet transformation, and the fusion experiment and quantitative evaluation of IKONOS, QuickBird, WordView-2 multi-spectral and panchromatic image show that the method has obvious advantages over traditional methods [5]. Wang Yanliang and Tang Yan discuss the remote sensing image fusion method based on multi-band wavelet transformation, and the experimental results show that the method not only improves the clarity and resolution of the image, but also retains the spectral information of the original image [6-7]. There are also some experts and scholars using single or multi-sensor image as the experimental data, and comparing the fusion effect of different algorithms from spectral fidelity and clarity of spatial structure information [8-12]. Various image fusion algorithms can achieve the complementation between spatial resolution and spectral resolution and improve the classification accuracy of remote sensing image, but different fusion algorithms have different advantages and limitations, so it is necessary to further study on what kind of fusion algorithm more conducive to improving the classification accuracy of remote sensing image. With IKONOS panchromatic and multi-spectral data as the object of study, this paper uses 5 algorithms (IHS, Brovey, PCA, SFIM, Gram-Schmidt) for image fusion and classification, and evaluates the image fusion effect in order to find the IKONOS image fusion algorithm suitable for land cover classification.

2 Image fusion algorithm and evaluation

2.1 Image fusion algorithm Pohl *et al.* believe that the most commonly used image fusion algorithm at present can be divided into color synthesis, arithmetic algorithm and image transformation [13], specifically including IHS transformation, Brovey transformation and PCA transformation. In recent years, the image

Received: November 22, 2014 Accepted: January 7, 2015
Supported by Chinese National Natural Science Foundation(51208016); Beijing Natural Science Foundation(8122008); Beijing Education Commission Fund (KM201310005023).
* Corresponding author. E-mail: jingxia1001@163.com

fusion algorithm of SFIM transformation [14], Gram-Schimdt transformation [15], Ehlers transformation [16] and pansharpening transformation [17] is also frequently reported.

2.1.1 IHS transformation. The IHS transformation can be realized using two methods. The first is the direct method, which transforms the 3-band image into the specified IHS space. The second is the alternative method, which firstly transforms a data set consisting of RGB3-band data into the separated IHS color space, then one of the components of IHS is replaced by another band image, and the fourth band image goes through the image enhancement processing, to obtain the same variance or mean as the image to be replaced. Finally, the fusion image is generated through the inverse transformation of IHS.

2.1.2 Brovey transformation. The Brovey transformation is also known as color standardization transformation. The multi-spectral band is firstly standardized, and then the standardized multi-spectral image is multiplied by high-resolution image to obtain the image after Brovey fusion. It is calculated as follows:

$$F_i = Pan \times M_i / \sum_{i=1}^{3} M_i (i = 1,2,3) \quad (1)$$

where F_i is the corresponding band data after fusion; Pan is the high-resolution panchromatic image data; M_i is one band of multi-spectral data.

2.1.3 Principal component analysis. Principal component analysis (PCA) is to reduce multiple components into several integrated components by the dimension reduction technique. Firstly, the principal component transformation is performed on the multi-spectral image, and then the high-resolution image is stretched to the same variance and mean as the first principal component; the stretched high-resolution image replaces the first principal component of multi-band image; finally, the image fusion is completed by the PCA inverse transformation on the replaced image. The direct transformation formula is as follows:

$$M_{PCA} = TM \quad (2)$$

where M_{PCA} is the multi-spectral image; M is the principal component image data obtained by the principal component transformation; T is the principal component transformation matrix obtained by calculating the covariance matrix of original multi-band image data.

The inverse transformation formula is as follows:

$$F = T^{-1} M_{PCA} \quad (3)$$

where F is the image data after fusion; M_{PCA} is the principal component image data after the first principal component is replaced; T^{-1} is the inverse transformation matrix of principal component.

2.1.4 Smoothing filter-based intensity modulation. The main step for smoothing filter-based intensity modulation (SFIM) [14] to perform image fusion is to first carry out strict registration of high-resolution images and low-resolution images, on this basis conduct neighborhood smoothing convolution operation of high-resolution images, and put the operation results as the median image. The transformation formula is as follows:

$$IMAGE_{SFIM} = \frac{IMAGE_{low} \times IMAGE_{high}}{IMAGE_{mean}} \quad (4)$$

where $IMAGE_{low}$ is the image obtained by resampling of low-resolution images on high-resolution images; $IMAGE_{mean}$ is the image obtained through the neighborhood smoothing convolution operation of high-resolution images; $IMAGE_{high}$ is the high-resolution image.

2.1.5 Gram-Schmidt transformation. The Gram-Schmidt transformation is to orthogonalize the matrix or multidimensional images to eliminate redundant information, and the key steps are as follows [15]: (i) using low spatial resolution multi-spectral images to simulate the high-resolution images; (ii) using the simulated high-resolution images as the first component of Gram- Schmidt transformation to carry out the Gram-Schmidt transformation of simulated high-resolution band images and low-resolution images; (iii) adjusting the statistical values of high-resolution images to match the first principal component GS1 after Gram-Schmidt transformation, in order to produce the modified high-resolution images; (iv) using the modified high-resolution images to replace the first component after Gram-Schmidt transformation to produce a new data set, and conducting inverse Gram-Schmidt transformation of new data set to produce the enhanced spatial resolution multi-spectral images.

2.2 Analysis and evaluation of image fusion effect The purpose of image fusion is to achieve complementarity between spatial resolution and spectral resolution, and minimize loss of the original information. The evaluation of its effect is often conducted on the basis of visual check combined with mathematical statistics method. The evaluation data selected in this paper is the IKONOS image of Shihezi City on July 25, 2008, and the basic information of experimental data is shown in Table 1.

Table 1 Basic information of experimental data

Data sources	IKONOS satellite image
Location	Shihezi
Acquisition time	July 25, 2008
Center latitude and longitude	44.5912°N 86.0987°E
Wave band	1 0.45 – 0.52 blue 2 0.52 – 0.60 green 3 0.63 – 0.69 red 4 0.76 – 0.90 near – infrared

2.2.1 Visual evaluation. For better comparison of visual effects of different fusion methods, this paper extracts some sub-sections from the whole scene image (Fig. 1). As can be seen from Fig. 1, the spatial resolution of image after fusion is significantly improved; the land and road borders are clear; the spatial texture information is greatly enhanced and details are more prominent. Although there are small differences in improving the spatial texture information between the five fusion algorithms, there are obvious differences in the information fidelity. The fidelity of SFIM fusion method is best, and the distortion of image obtained by IHS transformation is obvious.

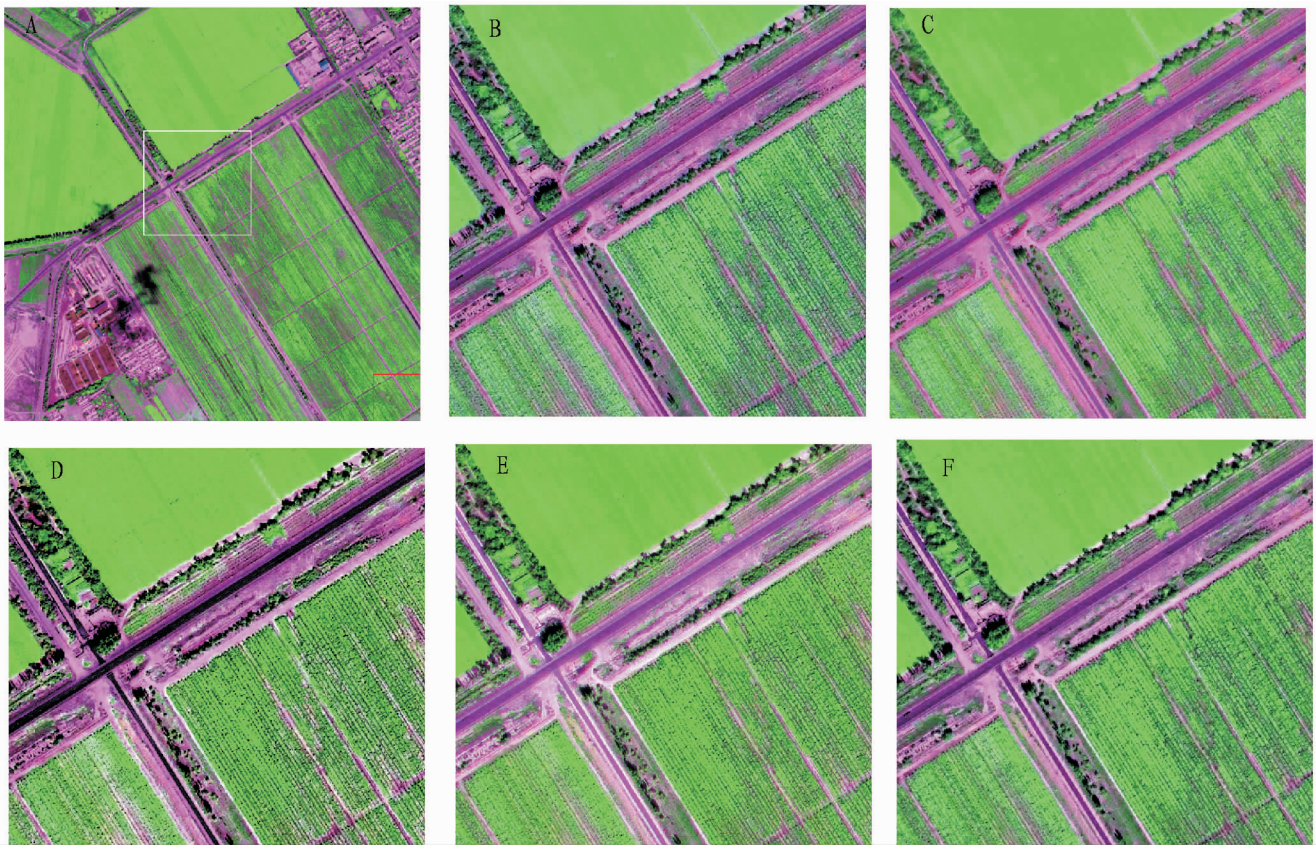

Note: A (IKONOS multi-spectral image); B (Brovey); C (Gram-Schmidt); D (IHS); E (PCA); F (SFIM).

Fig. 1 Fusion effect of IKONOS panchromatic and multi-spectral images

2.2.2 Quantitative analysis. The visual evaluation is susceptible to observers' experience and observing conditions, so this paper select 6 statistical parameters for measuring the amount of information (near-infrared band information entropy, average gradient, deviation index, correlation coefficient before and after fusion, mean and standard deviation) to conduct the quantitative analysis of spectral texture information enhancement and spectral information fidelity capacity. The statistical parameters are calculated in Table 2, and the quantitative evaluation results are shown in Table 3.

As can be seen from Table 3, the mean of image after IHS transformation and Brovey transformation is less than the mean of the original image. After the fusion using other transformation methods, the mean of image increases, and the mean for PCA fusion method increases most, so the image is brightest after PCA fusion. There is the smallest difference in the mean between the fusion image obtained through SFIM transformation and the original image, so from the mean evaluation indicator, the brightness of image after SFIM transformation fusion is consistent with the original image, and the fusion effect is most ideal. If regarding the information entropy of fusion image as the evaluation indicator for the quality of image fusion, the information entropy of fusion image obtained using 5 transformation methods is improved in varying degrees compared with the original image. From the deviation of the fusion image from the original image, the deviation index fusion image after IHS transformation is highest, indicating that the correlation between fusion image obtained through IHS transformation and the original image is lowest. The deviation index of SFIM transformation is smallest, followed by Gram-Schmidt transformation and Brovey transformation, indicating that the SFIM transformation keeps up the most spectral information of the original image. The average gradient indicates the relative clarity of image and reflects the texture richness of image after fusion. Table 3 shows that the ability of the 5 methods in this paper to express the details of ground object is improved, and there are great differences in the average gradient between the image after fusion using Gram-Schmidt transformation, PCA transformation or SFIM transformation, and the original image, especially for Gram-Schmidt transformation, indicating that Gram-Schmidt fusion algorithm has the strongest ability to express the contrast of tiny details of image, and the image clarity is better. From the correlation between the original image and the image after fusion, the fusion image after IHS transformation is least correlated with the original image, followed by Brovey transformation. The correlation coefficient between the original image and the fusion image after SFIM transformation, Gram-Schmidt transformation or PCA transformation is more than 0.9, indicating that there are great similarities in the spectral characteristics between the original image and the image

after fusion using the three methods, and spectral characteristics of the original image can be well kept.

Table 2 Calculation formula of various parameters

	Formula	
Information entropy	$H=\sum_{i=0}^{l-1}p_i\ln p_i$ where is the probability of level *i gray scale*.	Measuring the amount of information
Average gradient	$AG=\frac{1}{(m-1)\times(n-1)}\sum_{i=1}^{m-1}\sum_{j=1}^{n-1}\sqrt{\frac{(D(i,j)-D(i+i,j))^2+(D(i,j)-D(i,j+1))^2}{2}}$ where m is the number of rows of image; n is the number of columns of image; $D(i,j)$ is the DN value of image in row i and column j.	Reflecting the ability of image to express the contrast of tiny details
Deviation index	$D_k=\frac{1}{m}\sum_{i=1}^{m}\sum_{j=1}^{m}\frac{\lvert M(i,j)_k-M'(i,j)_k\rvert}{M(i,j)_k}$ where m is the number of rows of image; n is the number of columns of image; $M(i,j)_k$ is the pixel gray value of band k of the original image at (i, j).	Reflecting the degree of matching between fusion image and original image on the spectral information
Correlation coefficient	$CC_k=\frac{\sum_{i=1}^{m}\sum_{j=1}^{n}(M(i,j)_k-\overline{M_k})(M'(i,j)_k-\overline{M'_k})}{\sqrt{\sum_{i=1}^{m}\sum_{j=1}^{n}(M(i,j)_k-\overline{M_k})^2\sum_{i=1}^{m}\sum_{j=1}^{n}(M'(i,j)_k-\overline{M'_k})^2}}$ where m is the number of rows of image; n is the number of columns of image; CC is the correlation coefficient of brand k of image before and after fusion; $M(i,j)_k$ is the pixel gray value of band k of the original image at (i, j); $\overline{M_k}$ is the average gray value of band k; $M'(i,j)$ is the gray value of band k of the fusion image at (i, j); $\overline{M'_k}$ is the average gray value of band k of the fusion image.	Reflecting the similarity in spectral characteristics between fusion image and original image
Mean	$\overline{Z}=\frac{\sum_{i=1}^{M}\sum_{j=1}^{N}\overline{Z}(i,j)}{M\times N}$ where $Z(i, j)$ is the gray value of image at the coordinates (i, j).	Reflecting the average brightness of fusion image
Standard deviation	$\sigma=\sqrt{\frac{\sum_{i=1}^{M}\sum_{j=1}^{N}(Z(i,j)-\overline{Z})^2}{M\times N}}$ where $Z(i, j)$ is the gray value of image at the coordinates (i, j).	Reflecting the dispersion of image pixel gray value relative to the average gray value

Table 3 Quantitative evaluation of IKONOS multi-spectral and panchromatic band fusion results

	Mean	Standard deviation	Information entropy	Average gradient	Deviation index	Correlation coefficient
Original image	84.548	50.420	8.436	7.531		
IHS transformation	72.576	63.280	9.325	12.347	0.539	0.875
Brovey transformation	80.190	56.628	8.673	12.152	0.425	0.891
PCA transformation	95.658	57.045	9.531	14.846	0.478	0.913
SFIM transformation	84.604	60.453	9.646	15.079	0.307	0.907
Gram-Schmidt	91.846	60.735	9.795	17.037	0.358	0.918

Note: The statistics are collected based on the NIR band whole scene image before and after the fusion.

3 The classification accuracy evaluation of the image after fusion using different algorithms

For selecting the image fusion algorithm suitable for the land cover classification of remote sensing image, this paper firstly uses the maximum likelihood method to classify the fusion image after different transformation, and then uses confusion matrix to analyze the classification results for further accuracy evaluation of 5 image fusion algorithms.

3.1 Maximum likelihood classification The maximum likelihood method is a supervised classification algorithm commonly used in remote sensing image classification, with good statistical properties [18]. This paper firstly uses hand-held GPS to conduct field survey of different land use types within the study area to determine the samples for supervised classification, and then uses the maximum likelihood supervised classification method to classify the IKONOS fusion image after five kinds of transformation in accordance with four land cover types (road, shelter forest, cotton and grapes). The classification results are shown in Fig. 2, and we can find that the fusion image after Gram-Schmidt transformation and SFIM transformation has good classification effect, while the fusion image after IHS transformation has the worst classification effect.

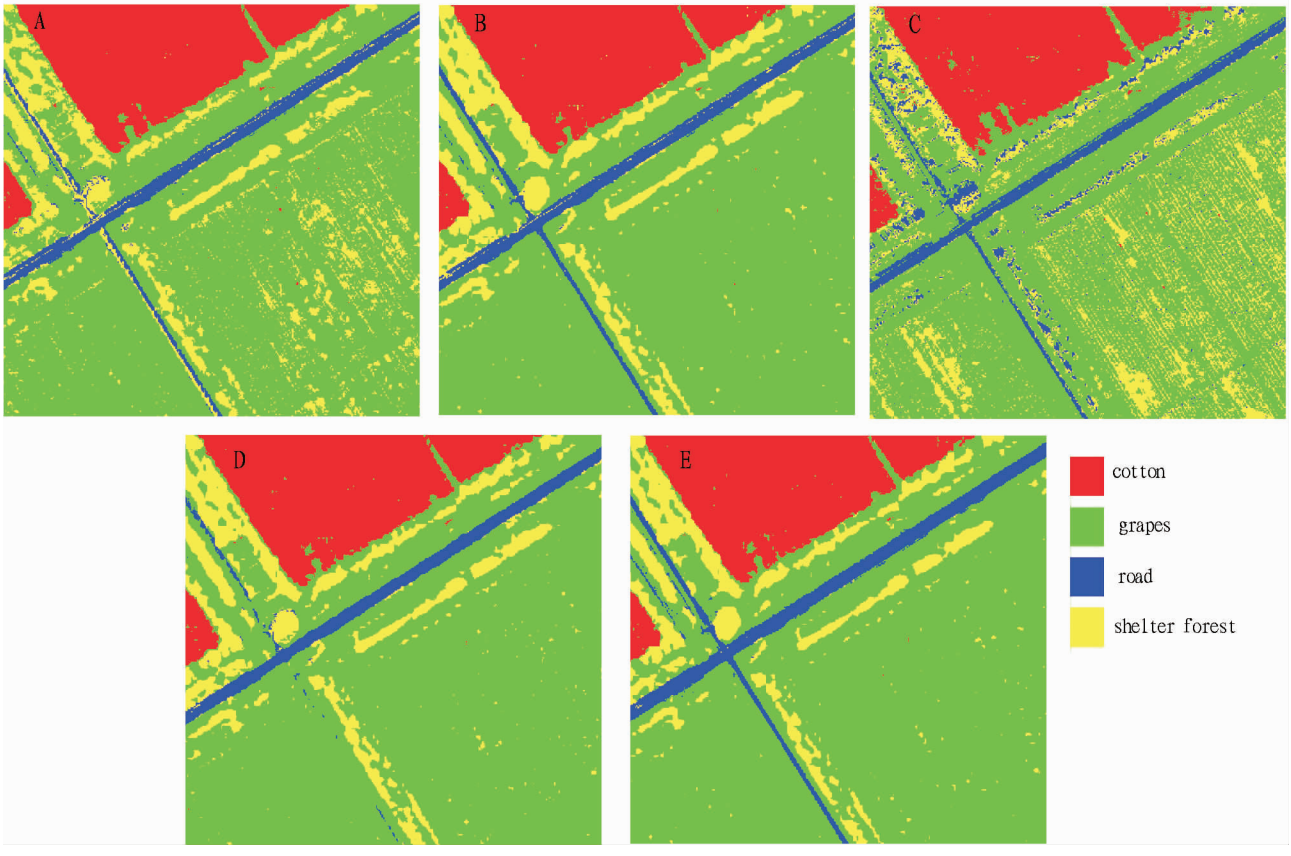

Note: A (Brovey); B (Gram-Schmidt); C (IHS); D (PCA); E (SFIM).

Fig. 2 The classification image of different fusion methods

3.2 Accuracy evaluation For more objective evaluation of the classification accuracy of different fusion algorithms, this paper uses the ground truth ROIs to establish the confusion matrix based on the field survey data, for calculating the overall accuracy of fusion image after different transformation and the Kappa coefficients (Table 4). As can be seen from Table 4, the land cover classification accuracy of fusion image by SFIM transformation and Gram-Schmidt transformation is high, and the overall classification accuracy is more than 98%. The classification accuracy of fusion image after Gram-Schmidt transformation is slightly better than that of fusion image after SFIM transformation; the classification accuracy of fusion image after IHS transformation is lowest, and the overall accuracy is only 83.14%.

Table 4 Evaluation of fusion image classification accuracy

Evaluation indicators	PCA	SFIM	Gram-Schmidt	Brovey	IHS
Overall accuracy (%)	94.07	98.60	98.95	92.09	83.14
Kappa coefficients	0.91	0.98	0.98	0.88	0.76

4 Conclusions and discussions

In this paper, with the IKONOS panchromatic and multi-spectral image as the object of study, we use five algorithms (IHS, Brovey, PCA, SFIM and Gram-Schmidt) for image fusion. We first use visual check and quantitative analysis to evaluate the image fusion results, then use the maximum likelihood method to classify the remote sensing image after fusion, and conduct the accuracy analysis of classification results on this basis. In terms of image spatial information improvement and spectral information fidelity, SFIM transformation and Gram-Schmidt transformation are better, and the Gram-Schmidt transformation has the stronger ability to express the contrast of tiny details of image than SFIM transformation, while in terms of spectral information fidelity, SFIM transformation is slightly better than Gram-Schmidt transformation. Among the five image fusion algorithms, the classification accuracy of fusion image obtained by Gram-Schmidt transformation is highest, and the overall accuracy and Kappa coefficient are 98.95% and 0.98, respectively. The classification accuracy of fusion image after Gram-Schmidt transformation is slightly better than that of fusion image after SFIM transformation; the classification accuracy of fusion image after IHS transformation is lowest, and the overall accuracy and Kappa coefficient are only 83.14% and 0.76, respectively. Therefore, the IKONOS fusion image obtained by Gram-Schmidt transformation and SFIM transformation is more conducive to improving the land cover classification accuracy. Among various image fusion algorithms, this paper only compares five algorithms and performs the qualitative and quantitative evaluation of image fusion effect based on specific object of study and purpose of application to select the best image fusion algorithm suitable for this study. However, there is a need to further verify

(To page 60)

state in recent 20 years of Dongting Lake[J]. Research of Environmental Sciences, 2013, 26(1): 27 -33. (in Chinese).
[4] RAO JP, YI M, FU Z, *et al*. Research on water quality changes in Dongting Lake[J]. Yueyang Vocational Technical College, 2011, 26(3): 53 -57. (in Chinese).
[5] ZHOU H, OU FP, LIU Y. The analysis of the water quality and its change trend of Dongting Lake during the period of" Eleventh Five - Year" [J]. Journal of Hunan Institute of Science and Technology (Natural Sciences), 2011, 24 (2): 88 -90. (in Chinese).
[6] LI YZ, LIU F, ZHANG CM. Analysis of change trend of water environment and cause in the Dongting Lake wetland[J]. Ecology and Environmental Sciences, 2011, 20 (8 -9): 1295 -1300. (in Chinese).
[7] CAO CS. Dynamics of water quality of East Dongting Lake and cause analysis[D]. Hunan Agricultural University, 2012. (in Chinese).
[8] DOU HS, JIANG JH. Dongting Lake[M]. Hefei: Press of University of Science and Technology of China, 2000. (in Chinese).
[9] ZHONG RL, BAO ZY, ZHOU X, *et al*. Temporal-spatial evolution of water quality in Lake Dongting, China[J]. Journal of Lake Science, 2007, 19 (6): 677 -682. (in Chinese).
[10] ZHANG JM, YU JQ, LIU Y. Analysis on eutrophication evaluation index and its evaluation of Lake Dongting[J]. Inland Fisheries, 2006, 31(2): 43 -44. (in Chinese).
[11] DAI SB, YANG SL, ZHU J, *et al*. The role of Lake Dongting in regulating the sediment budget of the Yangtze River[J]. Hydrology and Earth System Sciences, 2005, 9(6): 692 -698.
[12] XU KH, MILLIMAN JD. Seasonal variations of sediment discharge from the Yangtze River before and after impoundment of the Three Gorges Dam [J]. Geomorphology, 2009, 104(34): 276 -283.
[13] CHANG J, LI JB, LU DQ, *et al*. The hydrological effect between Jingjiang River and Dongting Lake during the initial period of Three Gorges Project operation [J]. Journal of Geographical Sciences, 2010, 20(5): 771 -786.
[14] LI JB, QIN JX, WANG KL, *et al*. The response of environment system changes of Dongting Lake to hydrological situation[J]. Acta Geographica Sinica, 2004, 59(2): 239 -248.
[15] WANG W, LU SY, JIN XC, *et al*. The spatial distribution of sediments and overilying water N of Dongting Lake[J]. Environmental Science & Technology, 2010, 33(12F): 6 -10. (in Chinese).
[16] LE C, ZHA Y, SUN D, *et al*. Eutrophication of lake waters in China: cost, causes, and control[J]. Environmental Management, 2010 (45): 662 -668.
[17] XIAO SY, TANG JC, HUANG X, *et al*. Analysis on agricultural non-point source pollution of Dongting Lake and countermeasures[J]. Agro-environment and Development, 2008, 25(3): 72 - 75. (in Chinese).
[18] LI JF. The monitoring, evaluation and control of agricultural non-point source pollution of Hunan Province[D]. Hunan Agricultural University, 2009. (in Chinese).
[19] CHEN XH. Water environment evaluation and planning[M]. Guangzhou: Sun Yat-sen University Press, 2001. (in Chinese).

(From page 56)

whether this conclusion is still tenable when considering more image fusion algorithms or using other classification methods.

References

[1] ZHOU QX, JING ZL, JIANG SZ. Comments on research and development of multi-source information fusion for remote sensing images[J]. Journal of Astronautics, 2002, 23(5): 89 -94. (in Chinese).
[2] ZHANG NY, WU QY. Information influence on QuickBird images by Brovey fusion and wavelet fusion[J]. Remote Sensing Technology and Application, 2006, 21(1): 67 -70. (in Chinese).
[3] LI CH, XU HQ. Spectral fidelity in high-resolution remote sensing image fusion[J]. Geo-Information Science, 2008, 10(4): 520 -526. (in Chinese).
[4] Kalpoma K A, Kudoh J. Image fusion processing for IKONOS 1-m color imagery[J]. IEEE Transactions on Geoscience and Remote Sensing, 2007, 45 (10): 3075 -3076.
[5] LIU J, LI DR, SHAO ZF. Fusion of remote sensing images based on fast discrete Curvelet transform[J]. Geomatics and Information Science of Wuhan University, 2011, 36(3): 333 -337. (in Chinese).
[6] WANG YL, TANG Y. Remote sensing image fusion based on multi-band wavelets[J]. Geomatics & Spatial Information Technology, 2010, 33(6): 16 -19. (in Chinese).
[7] TANG Y. Forest remote sensing image fusion based on multi-band wavelets [J]. Journal of Northeast Forestry University, 2010, 38(8): 68 -70. (in Chinese).
[8] QIU DH, WU YL, ZHANG RS. Fusion evaluation of Worldview-1 and SPOT5[J]. Journal of South west University (Natural Science Edition), 2010, 32(6): 168 -172. (in Chinese).
[9] ZHANG JW, SONG XD, YANG JA, *et al*. Comparison study on different fusion met hods based on ETM + image —A case study in Ansai and Yongshou County[J]. Journal of Northwest Forestry University, 2010, 25 (5): 152 -156. (in Chinese).
[10] LI JJ, HE LH, DAI JF, etal. Analysis of pixel-level remote sensing image fusion methods[J]. Geo-Information Science, 2008, 10(1):128 -134. (in Chinese).
[11] HAN SS, LI HT, GU HY. Study on image fusion for high spatial resolution remote sensing images[J]. Science of Surveying and Mapping, 2009, 34(5):60 -62. (in Chinese).
[12] Klonus S, Ehlers M. Performance of evaluation methods in image fusion [Z]. 12th International Conference on Information Fusion, Seattle, WA, USA, July 6 -9, 2009
[13] Pohl C,Van JLG. Multisensor image fusion in remote sensing: concepts, methods and applications[J]. International Journal of Remote Sensing, 1998, 19(5):823 -854.
[14] Liu JG. Smoothing filter-based intensity modulation: a spectral preserve image fusion technique for improving spatial details[J]. International Journal of Remote Sensing, 2000, 21(8): 3461 -3472.
[15] LI CG, LIU LY, WANG JH, *et al*. Comparison of two methods of fusing remote sensing images with fidelity of spectral information[J]. Journal of Image and Graphics, 2004, 9(11): 1376 -1387. (in Chinese).
[16] ZHAO ZM, MA W, WANG RS. Evaluation and analysis of three methods of fusing remote sensing images with high fidelity of spectral information [J]. Geology and Exploration, 2010, 46(4): 705 -710. (in Chinese).
[17] Ehlers M, Klonus S, strand PJ, etal. Multi-sensor image fusion for pan-sharpening in remote sensing[J]. International Journal of Image and Data Fusion, 2010, 1(1): 25 -45.
[18] TANG GA, ZHANG MS, LIU YM, *et al*. Digital remote sensing image processing[M]. Beijing: Science Press,2004:104 -107. (in Chinese).